Ternary Early-Transition-Metal Palladium Pnictides $Zr_3Pd_4P_3$, $Hf_3Pd_4P_3$, HfPdSb, and $Nb_5Pd_4P_4$

Meitian Wang, Robert McDonald,† and Arthur Mar*

Department of Chemistry, University of Alberta, Edmonton, Alberta, Canada T6G 2G2

Received June 16, 2000

Several ternary palladium pnictides of the early transition metals have been prepared by arc-melting of the elemental metals and the binary pnictides ZrP, HfP, $HfSb_2$, or NbP, and their structures have been determined by X-ray diffraction methods. The phosphides $M_3Pd_4P_3$ (M = Zr, Hf) adopt a new structure type (Pearson symbol *oP*40), crystallizing in the orthorhombic space group *Pnma* with $Z = 4$ and unit cell parameters of $a = 16.387(2)$, $b = 3.8258(5)$, and $c = 9.979(1)$ Å for $Zr_3Pd_4P_3$ and $a = 16.340(2)$, $b = 3.7867(3)$, and $c = 9.954(1)$ Å for $Hf_3Pd_4P_3$. The antimonide HfPdSb was identified by powder X-ray diffraction (orthorhombic, *Pnma*, $Z = 4$, $a = 6.754(1)$ Å, $b = 4.204(1)$ Å, and $c = 7.701(2)$ Å) and confirmed to be isostructural to ZrPdSb, which adopts the TiNiSi-type structure. The phosphide $Nb_5Pd_4P_4$ adopts the $Nb_5Cu_4Si_4$-type structure, crystallizing in the tetragonal space group *I*4/*m* with $Z = 2$, $a = 10.306(1)$ Å, and $c = 3.6372(5)$ Å. Coordination geometries of pentacapped pentagonal prisms for the early transition metal, tetracapped distorted tetragonal prisms for Pd, and tricapped trigonal prisms for the pnicogen are found in the three structures; tetracapped tetragonal prisms for Nb are also found in $Nb_5Pd_4P_4$. In common with many metal-rich compounds whose metal-to-nonmetal ratio is equal or close to 2:1, the variety of structures formed by these ternary palladium pnictides arises from the differing connectivity of pnicogen-filled trigonal prisms. Pnicogen−pnicogen bonds are absent in these structures, but metal−metal bonds (in addition to metal−pnicogen bonds) are important interactions, as verified by extended Hückel band structure calculations on $Zr_3Pd_4P_3$.

Introduction

Although many examples are now known of metal-rich binary and ternary transition-metal pnictides in which the ratio of metal to nonmetal is equal or close to 2:1,[1] by no means have they been exhaustively investigated, as demonstrated by the recent discovery of Hf_7P_4, for instance.[2] Their structures typically feature the pnicogen atoms coordinated in a trigonal prismatic fashion by the transition-metal atoms. The trigonal prisms may then be further capped on their quadrilateral faces by additional transition-metal atoms, leading to differentiation in structure types: monocapped in MoP_2-type, tricapped in TiNiSi-type, tetracapped in Co_2Si-type, and pentacapped in Ni_2In-type.[3] (A quadrilateral face can be capped by more than one atom, as occurs in the latter two cases.) There is extensive metal−pnicogen and metal−metal bonding in these structures but no pnicogen−pnicogen bonding. In ternary transition-metal pnictides containing a combination of an early and a late transition metal, metal−metal bonding can be understood in terms of a Lewis acid−base stabilization afforded by donation of electron density by the latter to the former.[4]

Among ternary pnictides $M_xM'_yPn_z$ (where M = Zr, Hf, Nb, Ta; M′ = Ni, Pd, Pt; Pn = P, As, Sb), there are numerous examples containing Ni,[5] but only recently have a few containing Pd ($Zr_5Pd_9P_7$, $Hf_5Pd_9P_7$, ZrPdAs, and ZrPdSb)[6] been reported and to date none is known with Pt. Paralleling these contrasts, the binary Ni and Pd phosphides share little in common; the

† Faculty Service Officer, Structure Determination Laboratory.

(1) Villars, P. *Pearson's Handbook, Desk Edition*; ASM International: Materials Park, OH, 1997.
(2) Kleinke, H.; Franzen, H. F. *Angew. Chem., Int. Ed. Engl.* **1996**, *35*, 1934.
(3) Hyde, B. G.; Andersson, S. *Inorganic Crystal Structures*; Wiley: New York, 1989.
(4) Kleinke, H. *Z. Anorg. Allg. Chem.* **1998**, *624*, 1771.
(5) (a) ZrNiP: Kuz'ma, Yu. B.; Paltii, Ya. F. *Russ. J. Inorg. Chem.* (*Engl. Transl.*) **1979**, *24*, 1421. (b) $ZrNiP_2$: El Ghadraoui, E. H.; Pivan, J. Y.; Guérin, R. *J. Less-Common Met.* **1988**, *136*, 303. (c) Zr_2NiP_2: El Ghadraoui, E. H.; Pivan, J. Y.; Guérin, R.; Sergent, M. *Mater. Res. Bull.* **1988**, *23*, 891. (d) Zr_4NiP_2: Bruskov, V. A.; Lomnitskaya, Ya. F.; Kuz'ma, Yu. B. *Sov. Phys. Crystallogr.* (*Engl. Transl.*) **1988**, *33*, 199. (e) $ZrNi_2P_2$: Lomnitskaya, Ya. F.; Kuz'ma, Yu. B. *Russ. J. Inorg. Chem.* (*Engl. Transl.*) **1986**, *31*, 1390. (f) $Zr_9Ni_2P_4$: Kleinke, H.; Franzen, H. F. *Inorg. Chem.* **1996**, *35*, 5272. (g) $Zr_2Ni_3P_3$ and $Hf_2Ni_3P_3$: El Ghadraoui, E. H.; Pivan, J. Y.; Guérin, R.; Padiou, J.; Sergent, M. *J. Less-Common Met.* **1985**, *105*, 187. (h) $ZrNi_4P_2$ and $HfNi_4P_2$: Pivan, J. Y.; Guérin, R.; El Ghadraoui, E. H.; Rafiq, M. *J. Less-Common Met.* **1989**, *153*, 285. (i) $Zr_2Ni_{17}P_7$ and $Zr_6Ni_{20}P_{13}$: Guérin, R.; El Ghadraoui, E. H.; Pivan, J. Y.; Padiou, J.; Sergent, M. *Mater. Res. Bull.* **1984**, *19*, 1257. (j) $Zr_{66}Ni_{17}P_{17}$, $Hf_{66}Ni_{17}P_{17}$, and $Ta_{66}Ni_{17}P_{17}$: Lomnitskaya, Ya. F.; Kuz'ma, Yu. B. *Inorg. Mater.* (*Engl. Transl.*) **1980**, *16*, 705. (k) HfNiP: Kleinke, H.; Franzen, H. F. *Z. Anorg. Allg. Chem.* **1996**, *622*, 1893. (l) $HfNi_xP$: Kleinke, H.; Franzen, H. F. *Z. Anorg. Allg. Chem.* **1996**, *622*, 1342. (m) Hf_2NiP: Kleinke, H.; Franzen, H. F. *Angew. Chem., Int. Ed. Engl.* **1997**, *36*, 513. (n) Hf_5NiP_3: Kleinke, H.; Franzen, H. F. *Chem. Mater.* **1997**, *9*, 1030. (o) NbNiP: Chaichit, N.; Chalugune, P.; Rukvichai, S.; Choosang, P.; Kaewchansilp, V.; Pontchour, C.-O.; Phavanantha, P.; Pramatus, S. *Acta Chem. Scand., Ser. A* **1978**, *32*, 309. (p) $NbNiP_2$: Kotur, B. Ya.; Lomnitskaya, Ya. F.; Kuz'ma, Yu. B. *Sov. Phys. Crystallogr.* (*Engl. Transl.*) **1983**, *28*, 348. (q) $Nb_2Ni_2P_3$: Guérin, R.; Potel, M.; Sergent, M. *J. Less-Common Met.* **1981**, *78*, 177. (r) Nb_2Ni_9P, Nb_3Ni_2P, and $Nb_{17}Ni_{50}P_{33}$: Lomnitskaya, Ya. F.; Kuz'ma, Yu. B. *Inorg. Mater.* (*Engl. Transl.*) **1983**, *19*, 1191. (s) Nb_4NiP: Paltii, Ya. F.; Kuz'ma, Yu. B. *Dopov. Akad. Nauk Ukr. RSR, Ser. A: Fiz.-Mat. Tekh. Nauki* **1977**, *39*, 262. (t) $Nb_5Ni_4P_4$ and $Ta_5Ni_4P_4$: Berger, R.; Phavanantha, P.; Mongkolsuk, M. *Acta Chem. Scand., Ser. A* **1980**, *34*, 77. (u) TaNiP: Rundqvist, S.; Nawapong, P. C. *Acta Chem. Scand.* **1966**, *20*, 2250. (v) $TaNiP_2$: El Ghadraoui, E. H.; Guérin, R.; Potel, M.; Sergent, M. *Mater. Res. Bull.* **1981**, *16*, 933.
(6) Heerdmann, A.; Johrendt, D.; Mewis, A. *Z. Anorg. Allg. Chem.* **2000**, *626*, 1393.

10.1021/ic0006551 CCC: $19.00
Published on Web 09/29/2000

only isostructural members are the phosphorus-rich compounds NiP_3 and PdP_3.[7,8] Besides these, Ni forms other phosphorus-rich compounds such as NiP_2[9] as well as metal-rich compounds (NiP,[9] Ni_2P (Fe_2P- and Ni_2P-types),[10,11] Ni_3P,[12] Ni_5P_2,[13] Ni_5P_4,[14] Ni_8P_3,[15] and $Ni_{12}P_5$[16]), whereas Pd forms only other metal-rich compounds (Pd_3P (Fe_3C-type),[17] Pd_6P,[18] Pd_9P_2,[19] $Pd_{15}P_2$,[20] Pd_7P_3[21]). More striking is the frequent lack of isotypy between the structures of ternary pnictides of Zr and Hf, ostensibly the two most similar elements in the periodic table. Differences in metal−metal bond strengths have been argued as the reason behind this observation,[22] although perhaps, in some cases, obtaining the desired phase may just be a matter of optimizing synthetic conditions.

In view of the surfeit of ternary nickel phosphides relative to the scarcity of ternary palladium phosphides, the metal-rich regions of the Zr, Hf, Nb, Ta/Pd/P systems were explored. The compounds $Zr_3Pd_4P_3$ and $Hf_3Pd_4P_3$ augment the recent discovery of $Zr_5Pd_9P_7$ and $Hf_5Pd_9P_7$,[6] and $Nb_5Pd_4P_4$ is the first compound found in this system. Also, the compound HfPdSb, isotypic with ZrPdSb,[6] has now been prepared.

Experimental Section

Synthesis. Binary transition-metal pnictides were first prepared by direct reaction of stoichiometric amounts of the elemental powders (Zr, 99.7%, Cerac; Hf, 99.8%, Cerac; Nb, 99.8%, Cerac; P, 99.995%, Cerac; Sb, 99.995%, Aldrich) in evacuated fused-silica tubes (3 days at 800 °C for ZrP and HfP, 3 days at 1000 °C for NbP, or 5 days at 650 °C for $HfSb_2$). Arc-melting reactions were then carried out on a 0.25-g scale on pressed pellets of mixtures of elemental Pd (99.95%, Cerac) and binary transition-metal pnictides, with the use of a Centorr 5TA triarc furnace under argon (gettered by melting a titanium pellet). Elemental compositions were determined by EDX (energy-dispersive X-ray) analysis on a Hitachi S2700 scanning electron microscope. Powder X-ray diffraction patterns were obtained on an Enraf-Nonius FR552 Guinier camera (Cu $K\alpha_1$ radiation, Si standard) and analyzed with the Filmscan and Jade 3.1 software packages.[23]

Small black needle-shaped crystals of $Zr_3Pd_4P_3$ were originally obtained from the reaction ZrP + 2Pd. EDX analysis revealed the presence of all three elements in the atomic proportions 27% Zr, 43% Pd, and 30% P in these crystals, one of which was selected for the structure determination. With a knowledge of the correct composition, $Zr_3Pd_4P_3$ was prepared with only trace amounts of unidentified impurity from the reaction 3ZrP + 4Pd. The analogous reaction 3HfP + 4Pd also afforded small black needle-shaped crystals of $Hf_3Pd_4P_3$, but the product was contaminated with ~30% binary impurities such as HfP. Similarly, small black plate-shaped crystals of $Nb_5Pd_4P_4$ were originally obtained from the reaction NbP + 2Pd. EDX analysis revealed the presence of all three elements in the atomic proportions 35% Nb, 35% Pd, and 30% P in these crystals, one of which was selected for the structure determination. The reaction Nb + 4NbP + 4Pd produced only about 50% $Nb_5Pd_4P_4$. Finally, the reaction Hf + 2Pd + $HfSb_2$ produced a black powder which was identified by X-ray diffraction to be ~80% HfPdSb, isostructural to ZrPdSb. Table 1 lists observed and calculated interplanar distances and intensities for HfPdSb.

Table 1. X-ray Powder Diffraction Data for HfPdSb[a]

hkl	$2\theta_{obs}$	d_{calc} (Å)	d_{obs} (Å)	I_c[b]	I_o
002	22.94	3.8506	3.8737	2	2
011	23.96	3.6898	3.7109	5	3
102	26.50	3.3452	3.3608	2	6
111	27.40	3.2381	3.2525	1	5
210	33.99	2.6328	2.6352	16	31
112	34.18	2.6175	2.6209	45	32
202	35.25	2.5390	2.5442	29	31
211	36.02	2.4912	2.4910	100	100
103	37.38	2.3996	2.4034	18	16
013	41.13	2.1909	2.1929	49	45
301	41.69	2.1610	2.1646	13	14
020	42.90	2.1018	2.1060	36	39
113	43.31	2.0840	2.0873	8	8
203	44.23	2.0437	2.0462	5	3
302	46.66	1.9436	1.9451	10	11
311	47.20	1.9219	1.9238	5	8
022	49.31	1.8449	1.8464	1	3
213	49.55	1.8380	1.8382	1	2
122	51.24	1.7797	1.7814	1	1
114	54.15	1.6944	1.6923	5	6
303		1.6926		3	
400	54.23	1.6886	1.6901	4	6
204	54.88	1.6726	1.6716	5	5
401	55.71	1.6494	1.6486	2	1
222	56.83	1.6191	1.6187	12	13
123	58.32	1.5811	1.5807	8	8
402	59.78	1.5464	1.5456	3	3
411	60.23	1.5354	1.5351	3	4
321	61.52	1.5067	1.5061	6	12
105	61.72	1.5017	1.5017	6	5
223	63.43	1.4652	1.4652	3	3
412	64.13	1.4513	1.4508	3	2
322	65.36	1.4270	1.4266	6	8
024	65.68	1.4197	1.4203	1	1
314	67.78	1.3819	1.3813	12	15
413	70.37	1.3374	1.3367	2	4
323	71.63	1.3183	1.3163	2	8
420		1.3164		3	
224	72.13	1.3088	1.3084	3	5
421	72.87	1.2976	1.2969	1	6
230	73.11	1.2942	1.2933	1	3
132		1.2924		3	
231	74.28	1.2763	1.2758	8	16
502		1.2747		1	
511	74.84	1.2685	1.2676	5	9
422	76.46	1.2456	1.2447	3	5
033	77.60	1.2299	1.2292	5	5
125	78.33	1.2219	1.2196	5	11
512		1.2198		2	
315	78.62	1.2168	1.2158	4	5
116	79.37	1.2078	1.2062	4	6

[a] The orthorhombic cell parameters refined from the powder pattern, obtained on a Guinier camera at room temperature with the use of the program POLSQ (program for least-squares unit cell refinement, modified by Cahen, D. and Keszler, D., Northwestern University, 1983), are $a = 6.754(1)$ Å, $b = 4.204(1)$ Å, $c = 7.701(2)$ Å, and $V = 218.66(8)$ Å^3. [b] The intensities were calculated based on positional parameters from the crystal structure of ZrPdSb (Heerdmann, A.; Johrendt, D.; Mewis, A. *Z. Anorg. Allg. Chem.* **2000**, *626*, 1393.) with the use of the program ATOMS (Dowty, E. *ATOMS*; Shape Software: Kingsport, TN, 1999).

Structure Determination. All crystals were prescreened by EDX analysis and Weissenberg photography. Intensity data were obtained

(7) Rundqvist, S.; Ersson, N.-O. *Ark. Kemi* **1968**, *30*, 103.
(8) Rundqvist, S. *Nature* (*London*) **1960**, *185*, 31.
(9) Larsson, E. *Ark. Kemi* **1965**, *23*, 335.
(10) Rundqvist, S. *Acta Chem. Scand.* **1962**, *16*, 992.
(11) Nowotny, H.; Henglein, E. *Z. Phys. Chem., Abt. B* **1938**, *40*, 281.
(12) Rundqvist, S.; Hassler, E.; Lundvik, L. *Acta Chem. Scand.* **1962**, *16*, 242.
(13) Chikhrii, S. I.; Kuz'ma, Yu. B. *Russ. J. Inorg. Chem.* (*Engl. Transl.*) **1990**, *35*, 1821.
(14) Elfström, M. *Acta Chem. Scand.* **1965**, *19*, 1694.
(15) Il'nitskaya, O. N.; Aksel'rud, L. G.; Mikhalenko, S. I.; Kuz'ma, Yu. B. *Sov. Phys. Crystallogr.* (*Engl. Transl.*) **1987**, *32*, 26.
(16) Rundqvist, S.; Larsson, E. *Acta Chem. Scand.* **1959**, *13*, 551.
(17) Andersson, Y.; Rundqvist, S.; Tellgren, R.; Thomas, J. O.; Flanagan, T. B. *J. Solid State Chem.* **1980**, *32*, 321.
(18) (a) Andersson, Y.; Kaewchansilp, V.; del Rosario Casteleiro Soto, M.; Rundqvist, S. *Acta Chem. Scand., Ser. A* **1974**, *28*, 797. (b) Andersson, Y.; Rundqvist, S.; Tellgren, R.; Thomas, J. O.; Flanagan, T. B. *Acta Crystallogr., Sect. B: Struct. Crystallogr. Cryst. Chem.* **1981**, *37*, 1965.
(19) Sellberg, B. *Acta Chem. Scand.* **1966**, *20*, 2179.
(20) Andersson, Y. *Acta Chem. Scand., Ser. A* **1977**, *31*, 354.
(21) Matković, T.; Schubert, K. *J. Less-Common Met.* **1977**, *55*, 177.
(22) Kleinke, H.; Felser, C. *J. Alloys Compd.* **1999**, *291*, 73.
(23) *Filmscan* and *Jade 3.1*; Materials Data Inc.: Livermore, CA, 1996.

Table 2. Crystallographic Data for $Zr_3Pd_4P_3$, $Hf_3Pd_4P_3$, and $Nb_5Pd_4P_4$

	$Zr_3Pd_4P_3$	$Hf_3Pd_4P_3$	$Nb_5Pd_4P_4$
formula mass (amu)	792.18	1053.98	1014.03
space group	D_{2h}^{16}–*Pnma* (No. 62)	D_{2h}^{16}–*Pnma* (No. 62)	C_{4h}^{5}–*I*4/*m* (No. 87)
a (Å)	16.387(2)[a]	16.340(2)[a]	10.306(1)[b]
b (Å)	3.8258(5)[a]	3.7867(3)[a]	10.306(1)[b]
c (Å)	9.979(1)[a]	9.954(1)[a]	3.6372(5)[b]
V (Å^3)	625.6(2)	615.9(1)	386.31(8)
Z	4	4	2
T (°C)	22	22	22
λ (Å)	0.71073	0.71073	0.71073
ρ_{calcd} (g cm^{-3})	8.410	11.367	8.717
μ(Mo Kα) (cm^{-1})	166.75	623.96	169.45
$R(F)$ for $F_o^2 > 2\sigma(F_o^2)$[c]	0.044	0.049	0.039
$R_w(F_o^2)$[d]	0.081	0.079	0.070

[a] Obtained from a refinement constrained so that $\alpha = \beta = \gamma = 90°$. [b] Obtained from a refinement constrained so that $a = b$ and $\alpha = \beta = \gamma = 90°$. [c] $R(F) = \sum||F_o| - |F_c||/\sum|F_o|$. [d] $R_w(F_o^2) = [\sum[w(F_o^2 - F_c^2)^2]/\sum wF_o^4]^{1/2}$; $w^{-1} = [\sigma^2(F_o^2) + (ap)^2 + bp]$ where $p = [\max(F_o^2,0) + 2F_c^2]/3$. For $Zr_3Pd_4P_3$, $a = 0.0223$ and $b = 0.0000$; for $Hf_3Pd_4P_3$, $a = 0.0135$ and $b = 0.0000$; for $Nb_5Pd_4P_4$, $a = 0.0238$ and $b = 0.0000$.

at 22 °C on a Bruker P4/RA/SMART 1000 CCD diffractometer using a combination of ϕ rotations (0.3°) and ω scans (0.3°) in the range $4° \le 2\theta(\text{Mo K}\alpha) \le 65°$ for $Zr_3Pd_4P_3$, $4° \le 2\theta(\text{Mo K}\alpha) \le 50°$ for $Hf_3Pd_4P_3$, and $5° \le 2\theta(\text{Mo K}\alpha) \le 65°$ for $Nb_5Pd_4P_4$. Crystal data and further details of the data collections are given in Table 2. All calculations were carried out using the SHELXTL (version 5.1) package.[24] Conventional atomic scattering factors and anomalous dispersion corrections were used.[25] Intensity data were processed, and face-indexed numerical absorption corrections were applied in XPREP. Initial atomic positions were found by direct methods using XS, and refinements were performed by least-squares methods using XL.

Weissenberg photographs of $Zr_3Pd_4P_3$ and $Hf_3Pd_4P_3$ revealed Laue symmetry *mmm* and systematic extinctions (0*kl*, $k + l = 2n + 1$; *hk*0, $h = 2n + 1$) consistent with the orthorhombic space groups *Pnma* and $Pn2_1a$. The centrosymmetric space group *Pnma* was chosen on the basis of the successful structure solution and refinement, which proceeded satisfactorily. Refinements on occupancy factors confirm that all sites are fully occupied. Although the structure determination of $Zr_3Pd_4P_3$ was straightforward, data collection for $Hf_3Pd_4P_3$ proved to be more challenging. Crystals that were singular (as revealed by Weissenberg photographs) and of suitable size were difficult to find; we made do with a small crystal of $Hf_3Pd_4P_3$ ($0.03 \times 0.005 \times 0.004$ mm) that had an even smaller fragment of HfP attached to it. Errors arising from the contribution of HfP to the collected intensities of $Hf_3Pd_4P_3$ were not serious because incidences of accidental overlap of reciprocal lattice points were low. The displacement parameters for the P atoms were refined isotropically; these were sensitive to absorption corrections, which are important even for such a small crystal because of the large absorption coefficient (μ(Mo Kα) = 624 cm^{-1}) but were difficult to apply because of imprecision in measuring the very small dimensions of the crystal. Final refinements led to satisfactory residuals (Table 2) and to featureless difference electron density maps ($\Delta\rho_{max} = 2.50$ and $\Delta\rho_{min} = -2.87$ e$^-$ Å^{-3} for $Zr_3Pd_4P_3$ and $\Delta\rho_{max} = 3.43$ and $\Delta\rho_{min} = -3.52$ e$^-$ Å^{-3} for $Hf_3Pd_4P_3$).

The possible space groups for $Nb_5Pd_4P_4$ consistent with its Laue symmetry 4/*m* and systematic extinctions indicating only body centering (*hkl*, $h + k + l = 2n + 1$) are *I*4, $I\bar{4}$, and *I*4/*m*. The centrosymmetric space group *I*4/*m* was chosen on the basis of its isotypy with $Nb_5Cu_4Si_4$ and the successful refinement (Table 2). The final difference electron map is featureless ($\Delta\rho_{max} = 2.37$ and $\Delta\rho_{min} = -2.03$ e$^-$ Å^{-3}).

The atomic positions of $Zr_3Pd_4P_3$, $Hf_3Pd_4P_3$, and $Nb_5Pd_4P_4$ were standardized with the program STRUCTURE TIDY.[26] Final values of the positional and displacement parameters are given in Table 3. Interatomic distances are listed in Table 4. Further data in the form of a CIF file are available as Supporting Information, and final structural amplitudes are available from the authors.

Table 3. Positional and Equivalent Isotropic Displacement Parameters for $Zr_3Pd_4P_3$, $Hf_3Pd_4P_3$, and $Nb_5Pd_4P_4$

atom	Wyckoff position	*x*	*y*	*z*	U_{eq} (Å^2)[a]
		$Zr_3Pd_4P_3$			
Zr(1)	4*c*	0.26016(9)	1/4	0.0244(2)	0.0051(3)
Zr(2)	4*c*	0.45161(9)	1/4	0.8825(2)	0.0050(3)
Zr(3)	4*c*	0.56056(9)	1/4	0.5893(2)	0.0050(3)
Pd(1)	4*c*	0.17653(7)	1/4	0.3107(1)	0.0066(3)
Pd(2)	4*c*	0.20644(7)	1/4	0.7352(1)	0.0064(3)
Pd(3)	4*c*	0.37095(7)	1/4	0.6170(1)	0.0061(2)
Pd(4)	4*c*	0.41869(7)	1/4	0.1833(1)	0.0063(3)
P(1)	4*c*	0.0448(2)	1/4	0.1795(4)	0.0056(7)
P(2)	4*c*	0.1141(2)	1/4	0.5366(4)	0.0055(8)
P(3)	4*c*	0.3227(2)	1/4	0.3888(4)	0.0065(8)
		$Hf_3Pd_4P_3$			
Hf(1)	4*c*	0.2602(1)	1/4	0.0229(2)	0.0044(5)
Hf(2)	4*c*	0.4522(1)	1/4	0.8810(2)	0.0061(5)
Hf(3)	4*c*	0.5605(1)	1/4	0.5880(2)	0.0093(5)
Pd(1)	4*c*	0.1765(2)	1/4	0.3104(4)	0.0041(8)
Pd(2)	4*c*	0.2058(2)	1/4	0.7310(4)	0.0023(7)
Pd(3)	4*c*	0.3703(2)	1/4	0.6176(4)	0.0041(7)
Pd(4)	4*c*	0.4194(2)	1/4	0.1825(4)	0.0051(8)
P(1)	4*c*	0.0428(6)	1/4	0.1801(12)	0.003(2)
P(2)	4*c*	0.1134(6)	1/4	0.5342(13)	0.007(3)
P(3)	4*c*	0.3233(6)	1/4	0.3883(12)	0.004(2)
		$Nb_5Pd_4P_4$			
Nb(1)	2*a*	0	0	0	0.0057(4)
Nb(2)	8*h*	0.3104(1)	0.3722(1)	0	0.0065(3)
Pd	8*h*	0.40535(8)	0.11385(9)	0	0.0073(2)
P	8*h*	0.0608(3)	0.2434(3)	0	0.0071(6)

[a] U_{eq} is defined as one-third of the trace of the orthogonalized $\mathbf{U}_{ij}$ tensor.

Band Structure. One-electron band structure calculations on $Zr_3Pd_4P_3$ were performed using the EHMACC suite of programs.[27,28] Extended Hückel parameters were taken from literature values and are listed in Table 5. Properties were extracted from the band structure using 120 *k* points in the irreducible portion of the Brillouin zone.

Results and Discussion

Although there are numerous ternary zirconium and hafnium nickel phosphides,[5a–n] none is isostructural to $Zr_3Pd_4P_3$ and $Hf_3Pd_4P_3$, which, along with the recently reported $Zr_5Pd_9P_7$ and $Hf_5Pd_9P_7$,[6] are the few examples of ternary zirconium and hafnium palladium phosphides known to date. $M_3Pd_4P_3$ (M = Zr, Hf) crystallizes in a new structure type; for concreteness we will take M = Zr in the following description. As in most ternary metal-rich phosphides, the unit cell has a short axis between 3 and 4 Å. A view of the structure down the short *b* axis is given in Figure 1. All atoms are located on mirror planes perpendicular to *b*, alternately on (x, $^1/_4$, z) or (x, $^3/_4$, z), as distinguished by the light or heavy lines. This representation emphasizes the description of the structure in terms of the stacking of two-dimensional nets consisting of triangles, distorted squares ("quadrangles"), and pentagons. These nets are self-dual,[29] with the vertexes of one net centering the polygons of the other net and vice versa.

(24) Sheldrick, G. M. *SHELXTL*, version 5.1; Bruker Analytical X-ray Systems, Inc.: Madison, WI, 1997.
(25) *International Tables for X-ray Crystallography*; Wilson, A. J. C., Ed.; Kluwer: Dordrecht, The Netherlands, 1992; Vol. C.
(26) Gelato, L. M.; Parthé, E. *J. Appl. Crystallogr.* **1987**, *20*, 139.
(27) Whangbo, M.-H.; Hoffmann, R. *J. Am. Chem. Soc.* **1978**, *100*, 6093.
(28) Hoffmann, R. *Solids and Surfaces*: *A Chemist's View of Bonding in Extended Structures*; VCH Publishers: New York, 1988.
(29) O'Keeffe, M.; Hyde, B. G. *Crystal Structures I. Patterns and Symmetry*; Mineralogical Society of America: Washington, DC, 1996.

Table 4. Selected Interatomic Distances (Å) for $Zr_3Pd_4P_3$, $Hf_3Pd_4P_3$, and $Nb_5Pd_4P_4$

		$Zr_3Pd_4P_3$	
Zr(1)−P(2)	2.814(3) (×2)	Zr(3)−P(1)	2.695(5)
Zr(1)−P(3)	2.708(3) (×2)	Zr(3)−P(1)	2.730(3) (×2)
Zr(1)−Pd(1)	3.047(2) (×2)	Zr(3)−P(3)	2.714(3) (×2)
Zr(1)−Pd(1)	3.168(2)	Zr(3)−Pd(2)	2.963(2)
Zr(1)−Pd(2)	2.896(2) (×2)	Zr(3)−Pd(3)	3.026(2) (×2)
Zr(1)−Pd(2)	3.017(2)	Zr(3)−Pd(3)	3.120(2)
Zr(1)−Pd(3)	3.022(2) (×2)	Zr(3)−Pd(4)	2.987(2) (×2)
Zr(1)−Pd(4)	3.044(2)	Zr(3)−Zr(3)	3.282(2) (×2)
Zr(1)−Zr(2)	3.442(2)	Pd(1)−P(1)	2.524(4)
Zr(1)−Zr(3)	3.462(2)	Pd(1)−P(2)	2.476(5)
Zr(2)−P(1)	2.787(3) (×2)	Pd(1)−P(3)	2.519(4)
Zr(2)−P(2)	2.680(3) (×2)	Pd(1)−Pd(2)	2.812(1) (×2)
Zr(2)−P(2)	2.782(4)	Pd(1)−Pd(3)	2.828(1) (×2)
Zr(2)−Pd(1)	2.930(2) (×2)	Pd(2)−P(2)	2.493(4)
Zr(2)−Pd(3)	2.961(2)	Pd(2)−P(3)	2.497(3) (×2)
Zr(2)−Pd(4)	2.934(2) (×2)	Pd(2)−Pd(3)	2.943(2)
Zr(2)−Pd(4)	3.050(2)	Pd(2)−Pd(4)	2.852(1) (×2)
Zr(2)−Zr(2)	3.416(3) (×2)	Pd(3)−P(1)	2.440(3) (×2)
Zr(2)−Zr(3)	3.428(2)	Pd(3)−P(3)	2.410(4)
		Pd(4)−P(1)	2.479(4)
		Pd(4)−P(2)	2.468(3) (×2)
		Pd(4)−P(3)	2.585(4)
		$Hf_3Pd_4P_3$	
Hf(1)−P(2)	2.804(8) (×2)	Hf(3)−P(1)	2.685(12)
Hf(1)−P(3)	2.691(8) (×2)	Hf(3)−P(1)	2.697(8) (×2)
Hf(1)−Pd(1)	3.021(3) (×2)	Hf(3)−P(3)	2.691(7) (×2)
Hf(1)−Pd(1)	3.171(4)	Hf(3)−Pd(2)	2.979(4)
Hf(1)−Pd(2)	2.861(3) (×2)	Hf(3)−Pd(3)	3.009(3) (×2)
Hf(1)−Pd(2)	3.038(4)	Hf(3)−Pd(3)	3.122(4)
Hf(1)−Pd(3)	3.003(3) (×2)	Hf(3)−Pd(4)	2.985(3) (×2)
Hf(1)−Pd(4)	3.048(4)	Hf(3)−Hf(3)	3.251(3) (×2)
Hf(1)−Hf(2)	3.442(3)	Pd(1)−P(1)	2.542(11)
Hf(1)−Hf(3)	3.443(3)	Pd(1)−P(2)	2.454(13)
Hf(2)−P(1)	2.755(9) (×2)	Pd(1)−P(3)	2.520(10)
Hf(2)−P(2)	2.657(8) (×2)	Pd(1)−Pd(2)	2.812(4) (×2)
Hf(2)−P(2)	2.766(11)	Pd(1)−Pd(3)	2.802(4) (×2)
Hf(2)−Pd(1)	2.916(3) (×2)	Pd(2)−P(2)	2.473(12)
Hf(2)−Pd(3)	2.943(4)	Pd(2)−P(3)	2.502(8) (×2)
Hf(2)−Pd(4)	2.896(3) (×2)	Pd(2)−Pd(3)	2.916(5)
Hf(2)−Pd(4)	3.049(4)	Pd(2)−Pd(4)	2.829(3) (×2)
Hf(2)−Hf(2)	3.411(3) (×2)	Pd(3)−P(1)	2.447(7) (×2)
Hf(2)−Hf(3)	3.411(3)	Pd(3)−P(3)	2.409(12)
		Pd(4)−P(1)	2.436(11)
		Pd(4)−P(2)	2.460(8) (×2)
		Pd(4)−P(3)	2.580(12)
		$Nb_5Pd_4P_4$	
Nb(1)−P	2.585(3) (×4)	Nb(2)−Nb(1)	2.9541(9) (×2)
Nb(1)−Nb(2)	2.9541(9) (×8)	Nb(2)−Nb(2)	3.292(2) (×2)
Nb(2)−P	2.572(2) (×2)	Nb(2)−Nb(2)	3.425(2) (×2)
Nb(2)−P	2.682(2) (×2)	Pd−P	2.365(2) (×2)
Nb(2)−P	2.919(3)	Pd−P	2.455(3)
Nb(2)−Pd	2.874(1) (×2)	Pd−Pd	2.822(1) (×4)
Nb(2)−Pd	2.885(1)	Pd−Pd	3.052(2)
Nb(2)−Pd	3.021(1)		

Table 5. Extended Hückel Parameters

atom	orbital	H_{ii} (eV)	ξ_{i1}	c_1	ξ_{i2}	c_2
Zr	5s	−8.93	1.82			
	5p	−5.29	1.78			
	4d	−9.24	3.84	0.6213	1.505	0.5798
Pd	5s	−7.51	2.19			
	5p	−3.86	2.15			
	4d	−12.53	5.98	0.55	2.61	0.67
P	3s	−18.60	1.88			
	3p	−12.50	1.63			

The Zr atoms occupy three crystallographically inequivalent sites, all having pentagonal prismatic coordination with each of the five quadrilateral faces further capped. This CN15 coordination is achieved by two Zr, nine Pd, and four P atoms surrounding Zr(1) and by four Zr, six Pd, and five P atoms surrounding Zr(2) or Zr(3). The four Pd sites have similar tetracapped distorted tetragonal prismatic coordination geometries (CN12), with Pd(1) showing the least severe distortion. Pd(1) is surrounded by five Zr, four Pd, and three P; Pd(2) by four Zr, five Pd, and three P; Pd(3) by six Zr, three Pd, and three P; and Pd(4) by six Zr, two Pd, and four P. If only Pd−P bonds are considered, then Pd(4) is found to be coordinated in a distorted tetrahedron of P atoms whereas the other Pd atoms are bonded to three P atoms in a T-shape (Pd(1)) or in a trigonal pyramid (Pd(2), Pd(3)). All P atoms reside at the centers of tricapped trigonal prisms. The CN9 coordination is completed by five Zr and four Pd around P(1) or P(2) and by four Zr and five Pd around P(3). The axial directions of the pentagonal, tetragonal, and trigonal prisms around Zr, Pd, and P atoms, respectively, are all oriented parallel to the *b* axis.

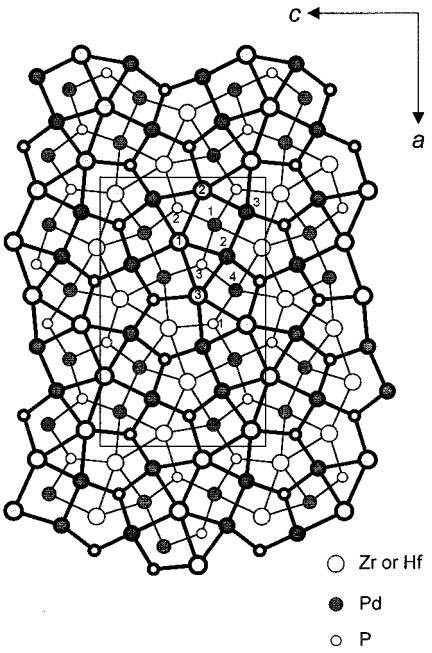

Figure 1. View of $Zr_3Pd_4P_3$ or $Hf_3Pd_4P_3$ in terms of two-dimensional nets stacked along the *b* axis at $y = 1/4$ (light lines) or $y = 3/4$ (heavy lines). The large lightly shaded circles are Zr or Hf atoms, the medium solid circles are Pd atoms, and the small open circles are P atoms.

The structures of most metal-rich transition-metal pnictides can be built up by considering pnicogen-centered trigonal prisms as building blocks. In $Zr_3Pd_4P_3$, each P-centered trigonal prism has four Zr and two Pd atoms at the vertexes and is linked with adjacent prisms through the two Zr−Zr edges to form a one-dimensional chain extending along the *a* direction, as shown in Figure 2a. Each trigonal prism also shares its two trigonal faces with adjacent prisms above and below along the *b* direction so that a two-dimensional corrugated sheet parallel to (001) results. Neighboring sheets are then translated by $1/2$ the *b* unit repeat, with the "notches" of one sheet fitting onto the "grooves" of the next sheet.

In a similar manner, Figure 2b shows that the structure of HfPdSb, isotypic with ZrPdSb,[6] also consists of chains of pnicogen-centered trigonal prisms, each having four Hf and two Pd atoms at the vertexes. (The coordination geometries around the other atoms in HfPdSb are also similar to those in $Zr_3Pd_4P_3$, with Hf atoms in pentacapped pentagonal prisms and Pd atoms in tetracapped distorted tetragonal prisms.) When the Sb-centered trigonal prisms are tricapped, as they are here, by additional metal atoms from adjacent chains, this is known as the TiNiSi-type structure,[30] an extremely common one. Among

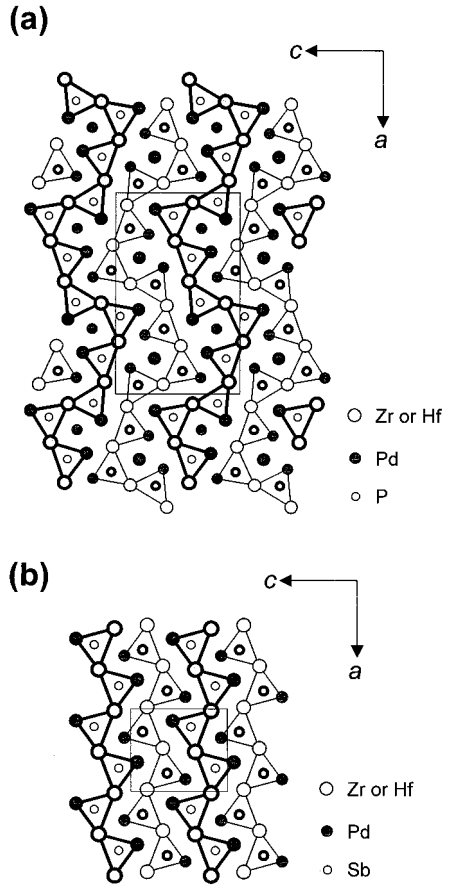

Figure 2. Comparison of the structures of (a) $Zr_3Pd_4P_3$ or $Hf_3Pd_4P_3$ and (b) ZrPdSb or HfPdSb, in terms of pnicogen-filled trigonal prisms, shown in projection down the *b* axis. Light and heavy lines indicate a displacement by $^1/_2$ the *b* unit repeat.

the ternary metal-rich pnictides $(M,M')_2Pn$, occasionally the structures are the same when a congeneric early transition metal is substituted (e.g., ZrPdSb (TiNiSi-type) vs HfPdSb (TiNiSi-type)[6]) but more frequently they differ subtly (e.g., ZrNiP (Ni_2-In-type with tetracapped trigonal prisms)[5a] vs HfNiP (TiNiSi-type)[5k]). The number of capping atoms around the trigonal prisms has been correlated with the height/base ratio of the trigonal prisms,[3] and for MPdSb and $M_3Pd_4P_3$ (M = Zr, Hf) these values (~1.2) are consistent with the presence of tricapped trigonal prisms, as indeed observed in their structures. In both structures, the trigonal prisms are linked exclusively through the edges containing the early transition metal (M−M) instead of the Pd−Pd edges to form the one-dimensional chains. Even with these restrictions, there are numerous possibilities for connecting these trigonal prisms to form different topologies and therefore different structures. In the case of $Zr_3Pd_4P_3$, whose metal-to-nonmetal ratio is close to 2:1, the trigonal prisms are connected in such a way as to create a new tetragonal prismatic site (Figure 2a) not present in $(M,M')_2Pn$ structures, which is occupied by an extra Pd atom.

In contrast with the ternary palladium phosphides ($Zr_3Pd_4P_3$, $Zr_5Pd_9P_7$) mentioned above, which find no counterparts in ternary nickel phosphides, the compound $Nb_5Pd_4P_4$ does turn out to be isostructural with the nickel analogues $Nb_5Ni_4P_4$ and $Ta_5Ni_4P_4$.[5t] (We have been unable to prepare "$Ta_5Pd_4P_4$" to date.) $Nb_5Pd_4P_4$ is the first ternary niobium palladium phosphide, and it adopts the $Nb_5Cu_4Si_4$-type structure,[31] an interesting one

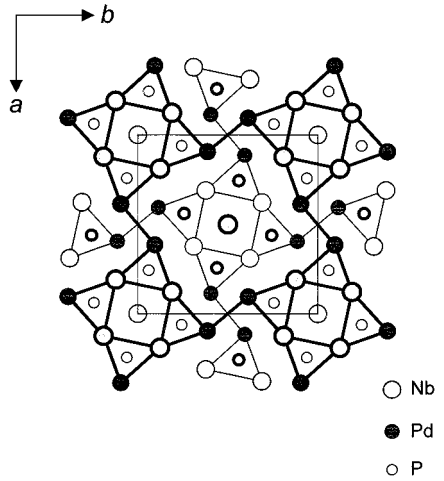

Figure 3. Structure of $Nb_5Pd_4P_4$ in terms of pnicogen-filled trigonal prisms, viewed in projection down the *c* axis. Light and heavy lines indicate a displacement by $^1/_2$ the *c* unit repeat.

which has been discussed widely.[32,33] The conventional description involves the condensation of Nb_6P_8 face-capped octahedral clusters through opposite vertexes to form one-dimensional chains which are linked via chains of edge-sharing tetrahedral Pd_4 clusters. However, as shown in Figure 3, the alternative description in terms of pnicogen-centered trigonal prisms emphasizes the close relationship with other ternary pnictides. Similar to the previous structures described, each P-centered trigonal prism has four Nb and two Pd atoms at the vertexes, with three additional capping atoms to form a tricapped trigonal prism. Four trigonal prisms are linked through Nb−Nb edges to form a tetrameric star-shaped cluster, generating a tetracapped tetragonal prismatic site occupied by Nb(1) (analogous to the tetragonal prismatic site occupied by Pd in $Zr_3Pd_4P_3$). Nb(2) resides in a pentacapped pentagonal prismatic site and Pd resides in a tetracapped distorted tetragonal prismatic site, as in the previous structures.

Although the use of pnicogen-centered trigonal prismatic building blocks clarifies structural relationships, little is implied about the relative importance of various bonding interactions other than the absence of pnicogen−pnicogen bonds in these structures. In all cases, metal−metal bonds, both homoatomic and heteroatomic, are undoubtedly important contributions in addition to metal−pnicogen bonds. These bonds extend in all three dimensions notwithstanding the portrayal of the structures in Figure 2; in fact, the interchain metal−metal bonds are shorter than the intrachain ones. The band structure for $Zr_3Pd_4P_3$ was therefore determined to assess these interactions. The density of states (DOS) curve (Figure 4) shows that although most of the Zr 4d states are above the Fermi level ($\epsilon_f = -9.55$ eV), a substantial portion is found to be mixing with Pd 4d and P 3p states in bonding levels below ϵ_f. Most of the Pd 4d states are found in the narrow peak between −11 and −13 eV, implying a d^{10} configuration for Pd. The calculated charges are +0.73 for Zr, −0.13 for Pd, and −0.56 for P. The Zr−P distances range from 2.680(3) to 2.814(3) Å, similar to those in Zr_2P (av 2.72 Å)[34] and $Zr_5Pd_9P_7$ (2.605(3)−2.803(3) Å)),[6] whereas the Pd−P distances range from 2.410(4) to 2.585(4) Å, similar to those in Pd_7P_3 (av 2.47 Å)[21] and $Zr_5Pd_9P_7$ (2.403(4)−2.684(5) Å).[6] Correspondingly, the crystal orbital overlap population (COOP)[35] curves (Figure 5a) confirm that the Zr−P bonding is

(30) Shoemaker, C. B.; Shoemaker, D. P. *Acta Crystallogr.* **1965**, *18*, 900.
(31) Ganglberger, E. *Monatsh. Chem.* **1968**, *99*, 549.
(32) Simon, A. *Angew. Chem., Int. Ed. Engl.* **1981**, *20*, 1.
(33) Simon, A. *Ann. Chim.* (*Paris*) **1982**, *7*, 539.
(34) Ahlzén, P.-J.; Rundqvist, S. *Z. Kristallogr.* **1989**, *189*, 117.

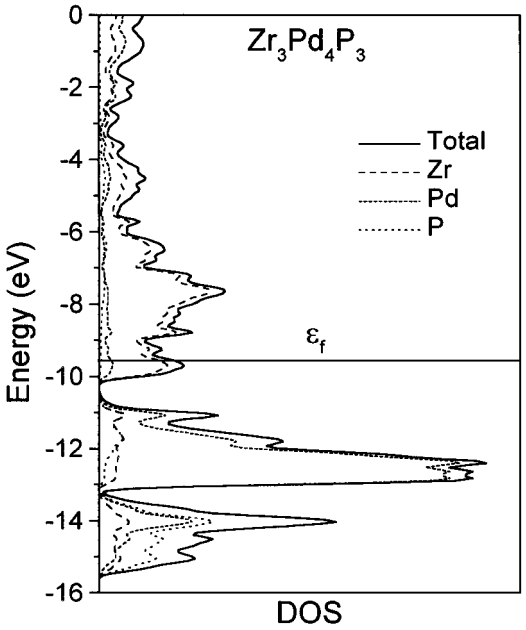

Figure 4. Density of states (DOS) curve for $Zr_3Pd_4P_3$ (solid line) and its Zr (long dashes), Pd (short dashes), and P (dotted) projections. The Fermi level, ϵ_f, is at −9.55 eV.

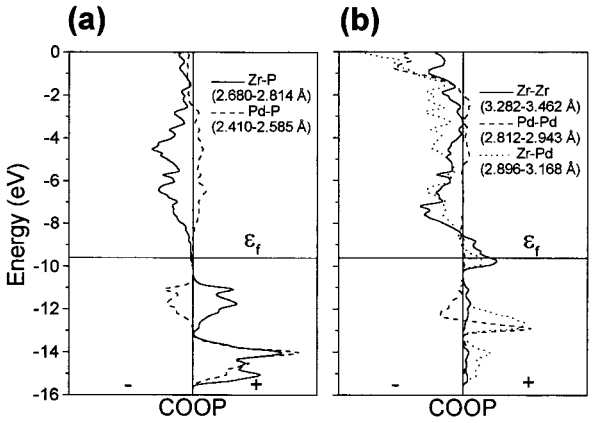

Figure 5. Crystal orbital overlap population (COOP) curves for the indicated (a) metal−P and (b) metal−metal contacts in $Zr_3Pd_4P_3$.

optimized with all bonding levels and no antibonding levels occupied (Mulliken overlap population (MOP) of 0.396), whereas the Pd−P bonding is moderately strong with some antibonding levels occupied (MOP of 0.148). The Zr−Zr distances range from 3.282(2) to 3.462(2) Å, slightly greater than those in elemental Zr (3.179−3.232 Å),[36] and the Pd−Pd distances range from 2.812(1) to 2.943(2) Å, longer than that in elemental Pd (2.751 Å).[36] The Zr−Pd distances of 2.896(2)−3.168(2) Å are comparable to those in Zr_3Pd_4 (2.774−3.059 Å)[37] and $Zr_5Pd_9P_7$ (2.898(2)−3.102(1) Å).[6] The COOP curves for these metal−metal interactions are shown in Figure 5b. Consistent with the reduced state of Zr, there is considerable Zr−Zr bonding with most of the bonding levels occupied and an MOP of 0.137. The small but positive MOP of 0.027 for the Pd−Pd contacts corresponds to a weak d^{10}−d^{10} interaction in which mixing with Pd 5s and 5p states further stabilizes bonding levels even though antibonding levels are occupied.[38] There may be other sources, such as dispersion, for this type of interaction, but the extended Hückel model suggests that such hybridization effects are important. Finally, the Zr−Pd bonding is essentially optimized with an MOP of 0.072, consistent with a Lewis acid−base stabilization implicit in interactions between early and late transition metals.

Whether the conclusions of the band structure calculation can be extrapolated to explain the absence of a "$Zr_3Ni_4P_3$" compound is questionable. Certainly d^{10}−d^{10} interactions will change on going to Ni, but covalent energies represent only one factor. The variety of ways that trigonal prisms can be connected to form different topologies suggests that energy differences between these structures may be quite small and subject to steric or matrix influences. As demonstrated in the synthesis of HfPdSb, which requires a higher temperature than that of ZrPdSb, the reason may be quite pedestrian: one simply has to look harder.

Acknowledgment. This work was supported by the Natural Sciences and Engineering Research Council of Canada and the University of Alberta. We thank Christina Barker (Department of Chemical and Materials Engineering) for assistance with the EDX analyses.

Supporting Information Available: An X-ray crystallographic file in CIF format for the structures of $Zr_3Pd_4P_3$, $Hf_3Pd_4P_3$, and $Nb_5Pd_4P_4$. This material is available free of charge via the Internet at http://pubs.acs.org.

IC0006551

(35) Hughbanks, T.; Hoffmann, R. *J. Am. Chem. Soc.* **1983**, *105*, 3528.
(36) Donohue, J. *The Structures of the Elements*; Wiley: New York, 1974.
(37) Bendersky, L. A.; Stalick, J. K.; Waterstrat, R. M. *J. Alloys Compd.* **1993**, *201*, 121.
(38) (a) Pyykkö, P. *Chem. Rev.* **1997**, *97*, 597. (b) Dedieu, A.; Hoffmann, R. *J. Am. Chem. Soc.* **1978**, *100*, 2074. (c) Mehrotra, P. K.; Hoffmann, R. *Inorg. Chem.* **1978**, *17*, 2187.